



# Kinetic modelling of testosterone-related differences in the hypothalamic–pituitary–adrenal axis response to stress

Ana Stanojević<sup>1</sup>  · Vladimir M. Marković<sup>1</sup> · Stevan Maćešić<sup>1</sup> · Ljiljana Kolar-Anić<sup>1,2</sup> · Vladana Vukojević<sup>3</sup> 

Received: 29 September 2017 / Accepted: 11 November 2017 / Published online: 17 November 2017  
© The Author(s) 2017. This article is an open access publication

**Abstract** The sex hormone testosterone (TTS) and the hypothalamic–pituitary–adrenal (HPA) axis mutually control one another’s activity, wherein TTS suppresses corticotrophin releasing hormone (CRH) stimulated HPA axis activity, whereas the activation of HPA axis has an inhibitory effect on TTS secretion. With an intention to explain these phenomena, a network reaction model is developed from the previously postulated stoichiometric models for HPA activity where main dynamic behaviors are controlled by two catalytic steps (one autocatalytic and one autoinhibitory) with respect to cortisol, both found experimentally. The capacity of the model to emulate TTS effects on HPA axis dynamics and its response to acute

---

**Electronic supplementary material** The online version of this article (<https://doi.org/10.1007/s11144-017-1315-7>) contains supplementary material, which is available to authorized users.

---

✉ Vladana Vukojević  
vladana.vukojevic@ki.se

Ana Stanojević  
ana.stanojevic@ffh.bg.ac.rs

Vladimir M. Marković  
vmarkovic@ffh.bg.ac.rs

Stevan Maćešić  
stevan.macesic@ffh.bg.ac.rs

Ljiljana Kolar-Anić  
ljiljana.kolar.anic@ffh.bg.ac.rs

- <sup>1</sup> Faculty of Physical Chemistry, University of Belgrade, Studentski trg 12-16, 11158 Belgrade, Serbia
- <sup>2</sup> Department of Catalysis and Chemical Engineering, Institute of Chemistry, Technology and Metallurgy, University of Belgrade, Njegoševa 12, 11000 Belgrade, Serbia
- <sup>3</sup> Department of Clinical Neuroscience, Center for Molecular Medicine CMM L8:01, Karolinska Institute, 17176 Stockholm, Sweden

CRH-induced stress is examined using numerical simulations. Model predictions are compared with empirically obtained results reported in the literature. Thus, the reaction kinetic examinations of nonlinear biochemical transformations that constitute the HPA axis, including the negative feedback effect of TTS on HPA axis activity, recapitulates the well-established fact that TTS dampens HPA axis basal activity, decreasing both cortisol level and the amplitude of ultradian cortisol oscillations. The model also replicates TTS inhibitory action on the HPA axis response to acute environmental challenges, particularly CRH-induced stress. In addition, kinetic modelling revealed that TTS induced reduction in ultradian cortisol amplitude arises because the system moves towards a supercritical Hopf bifurcation as TTS is being increased.

**Keywords** Autocatalysis and autoinhibition · Dynamic states of HPA axis · Kinetic modelling · Nonlinear dynamics · Stress · Testosterone

## Introduction

The hypothalamic–pituitary–adrenal (HPA) axis is a dynamical regulatory system that integrates and synchronizes the nervous and the endocrine systems actions at the organism level by self-regulating the circulating levels of peptide and steroid hormones produced by the hypothalamus, pituitary and adrenal glands [1–3]. This nonlinear system is characterized by a complex oscillatory dynamics of peptide and steroid hormones with two principal frequencies—ultradian oscillations with a period of 20–120 min that are superimposed on circadian oscillations with a period of about 24 h [4–6], which is essential for providing both a rapid response to stress and rapid relaxation to the normal state after a stressful challenge [7, 8].

The HPA axis-mediated stress response is initiated by the activation of several neural pathways that momentarily induce the synthesis and secretion of corticotrophin-releasing hormone (CRH) and subsequently the adrenocorticotrophic hormone (ACTH) that is released into the general blood circulation [9]. ACTH, in turn, stimulates the adrenal glands to produce and secrete steroid hormones [10–12]. In our previous work [13–19], which has originated from the pioneering work of Jelić et al. [20], we have shown that complex neurobiological processes and biochemical interactions that constitute the HPA axis can be effectively represented by a stoichiometric network of interactions and transformed into a kinetic model that allows us to use computerized numerical integration of a system of coupled ordinary differential equations (ODEs) to simulate complex changes in daily hormonal levels and make accurate predictions of HPA axis response to acute or chronic perturbations with internally present substances (ex. CRH [11, 12] and cholesterol [13, 17], with externally introduced substances (ex. ethanol [15]) or with non-substance disturbances (ex. electrical stimulations [16]). In all these variants of the model [11–18], basic reactions necessary to describe rhythmic dynamic changes are the same two feedback relations that concisely describe the experimentally well-established autocatalytic (R17) and autoinhibition (R18) feedback action of cortisol.

Together, these feedback loops form the core of this dynamic regulatory mechanism, with the positive feedback bringing forth excitability and propagation behavior and the negative feedback governing the recovery from these excited states.

The aim of this work is twofold: to further strengthen the predictive value of the stoichiometric network reaction model by including the experimentally established inhibitory effect of testosterone (TTS) on CRH-stimulated HPA axis activity [21]; and to assess the capacity of the newly developed model to emulate TTS-related differences in the HPA axis response to acute CRH-induced stress.

## Numerical procedures

The set of coupled ODEs describing the HPA axis dynamics and effects of perturbation with CRH is given in the Supplementary Material (Table S1).

Numerical simulations were performed using the MATLAB ode15 s solver that is based on the Gear algorithm for integration of stiff differential equations [22]. Absolute and relative error tolerance values were  $1 \times 10^{-20}$  and  $1 \times 10^{-14}$ , respectively. The model was integrated with stricter tolerances in order to minimize numerical artefacts, but the same dynamical behavior was observed using values of  $1 \times 10^{-9}$  and  $3 \times 10^{-6}$ .

Concentrations of 15 reaction species are considered as dynamical variables in the model: corticotrophin releasing hormone (CRH), adrenocorticotrophic hormone (ACTH), cortisol (CORT), aldosterone (ALDO), cholesterol (CHOL), pregnenolone (PNN), progesterone (PGS), deoxycorticosterone (DCTS),  $17\alpha$ -hydroxypregnenolone (HPNN),  $17\alpha$ -hydroxyprogesterone (HPGS), testosterone (TTS), Pro-opiomelanocortin (POMC),  $\beta$ -lipotropin ( $\beta$ -LPH),  $\beta$ -endorphin ( $\beta$ -END), melanocyte stimulating hormone-beta ( $\beta$ -MSH), as well as the melanocortin receptor type 2 ( $MC_2$ ) and its active form ( $MC_2^{active}$ ). Concentrations of all reaction species are expressed in moles per cubic decimeter ( $\text{mol}/\text{dm}^3 = \text{M}$ ). Initial conditions for the integration of ODEs in all numerical simulations are given in Table S2. Parameters in the circadian rhythm function D were  $d_1 = 0.3025$  and  $d_2 = 1.0$ .

To model the effect of TTS on HPA axis dynamics, the rate constant  $k_{30}$  (Table 1) was varied (Fig. 1). In order to facilitate comparison with data available in the literature, the average daily level of TTS was calculated for all values of rate constant  $k_{30}$  tested. These values are indicated on the upper abscissa in Figs. 1c and 1d, whereas the lower abscissa shows values of the actual independent variable, which is the rate constant  $k_{30}$ .

To simulate the effect of acute perturbations with CRH, numerical integration of the system of ODEs (Supplementary Material, Table S1) was stopped at a specified time point and new initial conditions for subsequent integration were defined. For the new initial conditions, CRH concentration was specified, while the concentrations of all other species retained their previously attained values. The relative change of cortisol amplitude after acute CRH ( $A_{rel}$ ) challenge was calculated as:

**Table 1** Stoichiometric model describing self-regulation of HPA axis hormones in humans (\*\*R1–R29) augmented with relations R30 and R31 to describe TTS production by Leydig cells in the testes or the thecal cells of female ovaries (R30) and the mutually negative effect of TTS and CRH (R31)

$\xrightarrow{k_1} \text{CHOL}$	$k_1 = 3.3120 \times 10^{-4} \text{ M min}^{-1}$	(R1)
$\xrightarrow{k_2 \times D} \text{CRH}$	$k_2 = 8.7840 \times 10^{-8} \text{ M min}^{-1}$	(R2)
$\xrightarrow{k_3} \text{ALDO}$	$k_3 = 1.4616 \times 10^{-10} \text{ M min}^{-1}$	(R3)
$\text{CRH} \xrightarrow{k_4} \text{POMC}$	$k_4 = 2.1960 \times 10^4 \text{ min}^{-1}$	(R4)
$\text{POMC} \xrightarrow{k_5} \text{ACTH} + \beta\text{LPH}$	$k_5 = 240.0000 \text{ min}^{-1}$	(R5)
$\beta\text{LPH} \xrightarrow{k_6} \beta\text{MSH} + \beta\text{END}$	$k_6 = 240.0000 \text{ min}^{-1}$	(R6)
$\text{ACTH} + \text{MC}_2 \xrightarrow{k_7} \text{MC}_2^{\text{active}}$	$k_7 = 7.6089 \times 10^{18} \text{ M}^{-1} \text{ min}^{-1}$	(R7)
$\text{MC}_2^{\text{active}} + \text{CHOL} \xrightarrow{k_8} \text{PNN} + \text{MC}_2$	$k_8 = 1.9022 \times 10^{10} \text{ M}^{-1} \text{ min}^{-1}$	(R8)
$\text{PNN} \xrightarrow{k_9} \text{HPNN}$	$k_9 = 15.4742 \text{ min}^{-1}$	(R9)
$\text{HPNN} \xrightarrow{k_{10}} \text{HPGS}$	$k_{10} = 7.7000 \text{ min}^{-1}$	(R10)
$\text{HPNN} \xrightarrow{k_{11}} \text{TTS}$	$k_{11} = 0.0371 \text{ min}^{-1}$	(R11)
$\text{HPGS} \xrightarrow{k_{12}} \text{CORT}$	$k_{12} = 0.0232 \text{ min}^{-1}$	(R12)
$\text{PNN} \xrightarrow{k_{13}} \text{PGS}$	$k_{13} = 0.2476 \text{ min}^{-1}$	(R13)
$\text{PGS} \xrightarrow{k_{14}} \text{CTS}$	$k_{14} = 0.2476 \text{ min}^{-1}$	(R14)
$\text{CTS} \xrightarrow{k_{15}} \text{ALDO}$	$k_{15} = 0.2352 \text{ min}^{-1}$	(R15)
$\text{PGS} \xrightarrow{k_{16}} \text{HPGS}$	$k_{16} = 1.0000 \times 10^{-4} \text{ min}^{-1}$	(R16)
$\text{HPGS} + 2 \text{ CORT} \xrightarrow{k_{17}} 3 \text{ CORT}$	$k_{17} = 3.0240 \times 10^{12} \text{ M}^{-2} \text{ min}^{-1}$	(R17)
$\text{ALDO} + 2 \text{ CORT} \xrightarrow{k_{18}} \text{CORT}$	$k_{18} = 1.6920 \times 10^{13} \text{ M}^{-2} \text{ min}^{-1}$	(R18)
$\text{CRH} + \text{CORT} \xrightarrow{k_{19}}$	$k_{19} = 7.2000 \times 10^{10} \text{ M}^{-1} \text{ min}^{-1}$	(R19)
$\text{ACTH} + \text{CORT} \xrightarrow{k_{20}}$	$k_{20} = 6.0000 \times 10^8 \text{ M}^{-1} \text{ min}^{-1}$	(R20)
$\text{ACTH} \xrightarrow{k_{21}}$	$k_{21} = 1.2840 \times 10^3 \text{ min}^{-1}$	(R21)
$\text{ALDO} \xrightarrow{k_{22}}$	$k_{22} = 0.8100 \text{ min}^{-1}$	(R22)
$\beta\text{END} \xrightarrow{k_{23}}$	$k_{23} = 2.4000 \times 10^3 \text{ min}^{-1}$	(R23)
$\beta\text{MSH} \xrightarrow{k_{24}}$	$k_{24} = 2.4000 \times 10^4 \text{ min}^{-1}$	(R24)
$\text{CHOL} \xrightarrow{k_{25}}$	$k_{25} = 0.1080 \text{ min}^{-1}$	(R25)
$\text{CORT} \xrightarrow{k_{26}}$	$k_{26} = 0.0984 \text{ min}^{-1}$	(R26)

**Table 1** continued

$\text{CRH} \xrightarrow{k_{27}}$	$k_{27} = 0.0013 \text{ min}^{-1}$	(R27)
$\text{PNN} \xrightarrow{k_{28}}$	$k_{28} = 0.0257 \text{ min}^{-1}$	(R28)
$\text{TTS} \xrightarrow{k_{29}}$	$k_{29} = 12.0000 \text{ min}^{-1}$	(R29)
$\xrightarrow{k_{30}} \text{TTS}$	$k_{30} = 2 \times 10^{-7} \text{ M min}^{-1} \text{ a}$	(R30)
	$k_{30} = 2 \times 10^{-8} \text{ M min}^{-1} \text{ b}$	
$\text{TTS} + \text{CRH} \xrightarrow{k_{31}}$	$k_{31} = 5 \times 10^{10} \text{ M}^{-1} \text{ min}^{-1}$	(R31)

Relations (R1–R29) and corresponding kinetic rate constants  $k_1$ – $k_{29}$  are the same as in Čupić et al. Addict. Biol. 2016 May 18. <https://doi.org/10.1111/adb.12409>

Some rate constants critically affect the HPA axis dynamics, requiring a larger number of significant figures, whereas others do not. For uniformity, the same number of digits is used for all rate constants, however the trailing zeroes do not imply a high sensitivity to variations in the parameter

<sup>a</sup>Individuals with high TTS levels

<sup>b</sup>Individuals with low TTS levels

$$A_{rel} = \frac{A}{A_0}, \tag{1}$$

Here  $A_0$  denotes amplitude of a reference ultradian CORT oscillation under basal, i.e. unperturbed conditions, whereas  $A$  denotes the resulting amplitude of the same reference ultradian CORT oscillation after acute perturbation with CRH (Fig. S1). The reference ultradian cortisol oscillation was arbitrarily selected as the first ultradian oscillation commencing after the time point of perturbation [14].

To model the effect of chronic stress, the rate constant  $k_2$  (Table 1) was varied in order to alter CRH levels (as described in detail in [14]).

## Results

### Development of the kinetic model

In order to describe the feedback effects of TTS on HPA axis dynamics, we started by building further on previously postulated variants of stoichiometric network models describing HPA axis activity [13–17], where the main dynamic behaviors are controlled by one autocatalytic and one autoinhibitory step with respect to cortisol. Although all these variants briefly describe biochemical transformations underlying the HPA axis in humans, a recently published variant [17] with 17 species was selected as the basis for further development because all dynamical variables are in physiological range in this model [15]. Biological and biochemical arguments for the development of the stoichiometric network are briefly summarized in the Supplementary Material (section Stoichiometric model describing the HPA axis). Here we would only like to underline that the precursor model developed by Čupić et al. (Table 1, R1–R29) includes TTS as a dynamical variable,

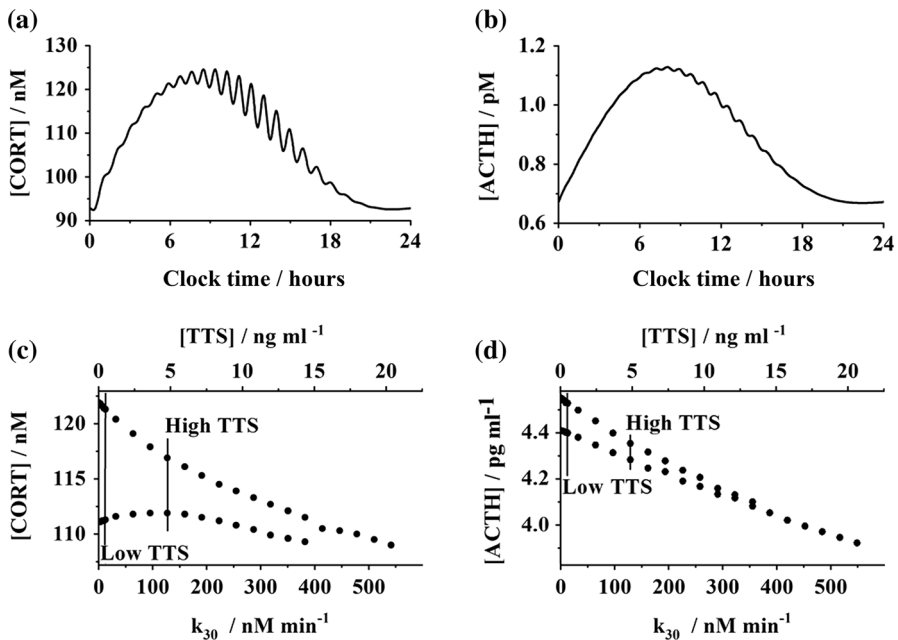


**Fig. 1** Kinetic modelling of TTS effects on HPA axis dynamics. Time evolution of: **a** CORT and **b** ACTH concentration during 24 h for  $k_{30,low} = 2 \times 10^{-8} \text{ M min}^{-1}$ , i.e. for a low TTS value. Bifurcation diagram showing changes in: **c** the largest ultradian CORT amplitude and **d** the largest ultradian ACTH amplitude as a function of the rate constant  $k_{30}$ . In order to facilitate comparison with data available in the literature, the average daily level of TTS was calculated, expressed in  $\text{ng ml}^{-1}$  and indicated on the upper abscissa. The concentration conversion factor for CORT is  $1 \text{ ng ml}^{-1} = 3.47 \text{ nmol dm}^{-3}$

but only accounts for its production in the adrenal glands (reaction R11) and its subsequent removal and/or biochemical transformation (reaction R29), and does not consider the mutually negative effect of TTS on the HPA axis activity and the inhibitory effect of HPA axis activation on testosterone secretion. In order to take into consideration TTS feedback effects on the HPA axis, we have augmented this model with two relations (Table 1). Relation R30 succinctly describes the production of testosterone outside the HPA axis, in particular the testosterone biosynthesis by Leydig cells in the male testes or by the thecal cells of female ovaries and its secretion in the peripheral blood circulation [21]. In order to model individual differences in TTS levels, which are obviously different for males and females but differ also between individuals of the same gender, the rate constant  $k_{30}$  in relation R30 assumes a low value for individuals with low TTS levels ( $k_{30,low} = 2 \times 10^{-8} \text{ M min}^{-1}$ ), as compared to individuals with high TTS levels ( $k_{30,high} = 2 \times 10^{-7} \text{ M min}^{-1}$ ). Relation R31 briefly describes the mutually negative bidirectional interaction between TTS and the HPA axis, wherein TTS suppresses CRH-stimulated HPA axis activity whereas activation of HPA axis has an inhibitory effect on testosterone secretion [22].

The corresponding set of ordinary differential equations (ODEs) describing the temporal evolution of the concentration of all species that are included in the stoichiometric network model in Table 1 is given in Table S1, and the initial conditions for numerical integration are presented in Table S2. Reference values of physiological concentrations of total testosterone in the blood compared to the values obtained by numerical simulation are given in Table 2. Normal basal blood levels of cholesterol and all peptide and steroid hormones as compared to the values determined by kinetic modelling using the stoichiometric network model in Table 1 are summarized in Table S3.

The capacity of this reaction kinetic model to emulate TTS effects on HPA axis dynamics and its response to acute and chronic CRH-induced stress is further examined.

### Testosterone reduces basal cortisol level and dampens HPA axis ultradian oscillations

In agreement with experimental observations [21, 23, 24], the kinetic modelling shows that TTS decreases basal CORT (Figs. 1a and 1c) and ACTH (Figs. 1b and 1d) levels and reduces the amplitude of ultradian CORT and ACTH oscillations (Fig. 1).

Furthermore, the model predicts that for both, low (Fig. 2a) and high (Fig. 2b) value of the rate constant  $k_{30}$ , TTS (grey) follows CORT (black) oscillations and that both reach the circadian peak almost simultaneously (Figs. 2a and 2b), in agreement with experimental findings recently reviewed by Hayes et al. [25].

Finally, the model also replicates complex daily changes in the ratio of TTS over CORT levels (Fig. 2c), in agreement with experimental observations by Duke et al. [26].

### Testosterone dampens the HPA axis response to acute CRH-induced stress but does not significantly affect its response to chronic stress

The HPA axis response to CRH-induced perturbations depends on the TTS concentration, the intensity of the perturbation and the phase of ultradian oscillation at which the perturbation is applied (Figs. 3 and 4). Thus, for both, low (Figs. 3a–3e) and high (Figs. 3f–3j) TTS levels, acute CRH-induced stress of the same

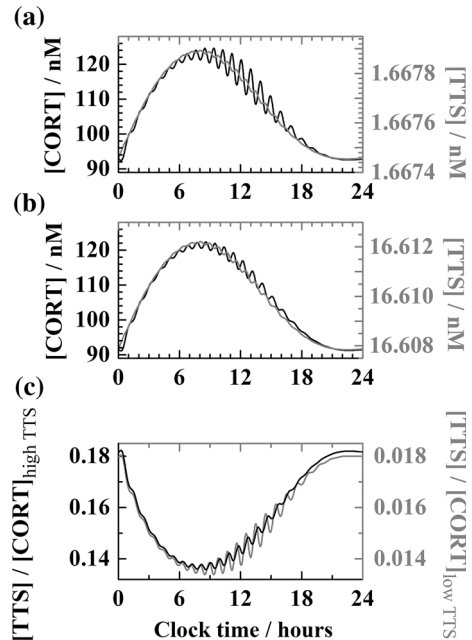
**Table 2** Reference values of physiological concentrations of total testosterone in the blood and the values obtained by numerical simulation

Individual differences in TTS levels	Reference physiological TTS value <sup>a</sup> (ng ml <sup>-1</sup> )	TTS concentration in numerical simulations (ng ml <sup>-1</sup> )
Low TTS level	0.1–1.2	0.48
High TTS level	2.4–12	4.78

Concentration conversion factor: 1 ng ml<sup>-1</sup> = 3.47 nmol dm<sup>-3</sup>

<sup>a</sup>Mayo Medical Laboratories

**Fig. 2** Kinetic modelling of TTS effects on daily changes in the TTS to CORT ratio. Circadian and ultradian oscillations of cortisol (black curve with large-amplitude ultradian oscillations) and testosterone (grey curve with low-amplitude ultradian oscillations) predicted by the model in Table 1 for: **a**  $k_{30,low} = 2 \times 10^{-8} \text{ M min}^{-1}$ , i.e. for low TTS level and **b**  $k_{30,high} = 2 \times 10^{-7} \text{ M min}^{-1}$ , i.e. high TTS level. All other parameters are as given in Table 1. **c** Daily variation in (TTS)/[CORT] ratio for low TTS level (grey curve with large-amplitude oscillations) and for high TTS level (black curve with low-amplitude oscillations)



intensity, modelled as an instantaneous surge in CRH level [13], elicits different changes in the ultradian cortisol amplitude when the perturbation is induced in a different phase of an ultradian oscillation: CORT minimum, CORT maximum, and two inflection points between them (Figs. 3b–3e, 3g–3j and 4a). The complex dependence of  $A_{rel} = A/A_0$  (as defined by Eq. 1) on the phase of the ultradian oscillation at which an acute CRH surge is induced (Fig. 4a), clearly shows that the actual HPA axis response to acute CRH-induced stress is coupled to the innate ultradian rhythmicity and the actual response critically depends on whether the perturbation was introduced during the predominance of CORT-producing or CORT-degrading pathways.

Moreover, reaction kinetic modelling shows that acute CRH-induced stress of the same intensity and the same time of onset, elicits different responses when TTS is high than when it is low (Figs. 4b and 4c). As expected, the behavior of the HPA axis when TTS is low is very similar to the referent state, when the feedback action of TTS is not considered in the model, i.e. in the model without relations R30 and R31 (Figs. 4b and 4c, squares vs. triangles). However, when TTS is high, the HPA axis response to acute CRH-induced stress is markedly different (Figs. 4b and 4c, crosses vs. triangles/squares).

Fig. 4b shows how the ratio  $A_{Max}/A_{0,ref}$  changes when the intensity of CRH-induced stress increases. Here,  $A_{Max}$  is the amplitude of a selected ultradian CORT oscillation after a perturbation is applied at the maximum of CORT concentration, and  $A_{0,ref}$  is the amplitude of the corresponding CORT ultradian oscillation in an unperturbed HPA axis without TTS feedback (i.e. in a model without relations R30 and R31). Thus, we compare the elicited effect relative to the same reference



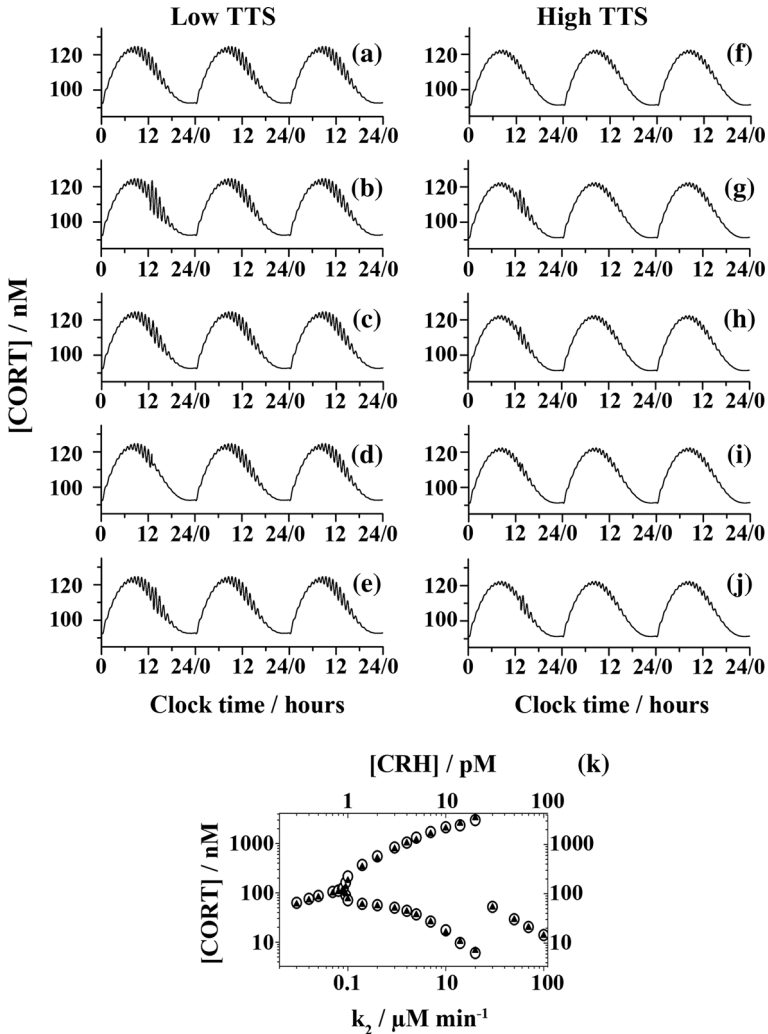


**Fig. 3** Kinetic modelling of testosterone effect on HPA axis response to acute and chronic CRH-induced stress. **a–j** Time series showing HPA axis response to acute CRH-induced challenge for low (**a–e**) and high (**f–j**) testosterone level, when the system is unperturbed (**a, f**) and when the CRH challenge is elicited at a specific point under an ultradian oscillation: at cortisol minimum (**b, g**), downward inflection point (**c, h**), cortisol maximum (**d, i**) and upward inflection point (**e, j**). **k** Bifurcation diagram showing the effect of low TTS (circles) and high TTS (triangles) levels on chronic CRH-induced stress

amplitude ( $A_{0,ref}$ ). As can be seen, the effect of an instantaneous CRH-induced perturbation on HPA axis dynamics depends on both, the intensity of the perturbation and the average TTS level (Fig. 4b, crosses vs. triangles/squares).

In order to gain more insight into this interdependence, we have analyzed the relative effect of CRH-induced stress,  $A_{Max}/A_0$ , where  $A_{Max}$  is, as above, the amplitude of a selected ultradian CORT oscillation after a perturbation is applied at the maximum of CORT concentration and  $A_0$  is the amplitude of the respective

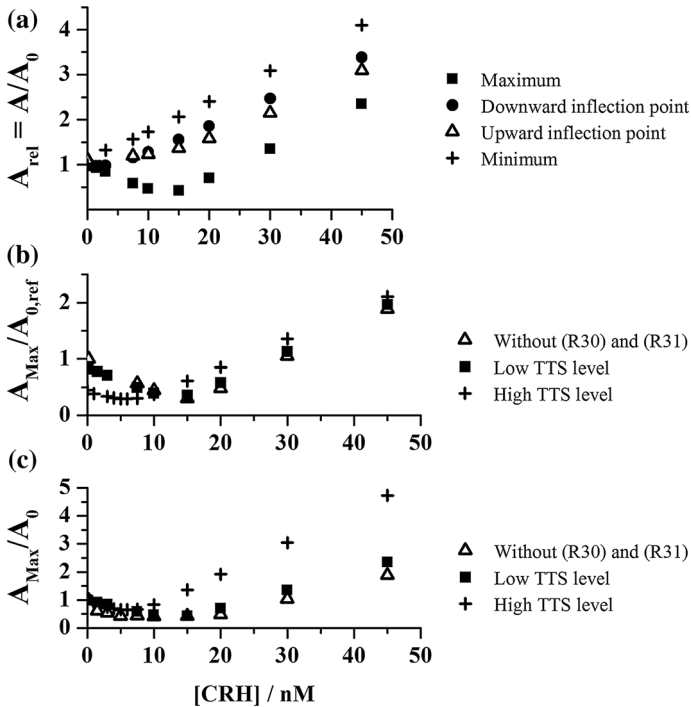


**Fig. 4** Differential HPA axis response to acute CRH-induced stress when average daily TTS concentration is high or low. **a** Relative change in the ultradian CORT amplitude (Eq. 1) as a function of the intensity of an instantaneous CRH-induced perturbations applied at CORT maximum (square), CORT minimum (crosses) and the upward (triangles) and downwards (dots) inflection points. The minima of the curves correspond to the maximal quenching of the ultradian oscillations, which depends on the phase of the oscillation as well as on TTS concentration. **b** The ratio  $A_{Max}/A_{0,ref}$  as a function of the intensity of CRH-induced stress. Here  $A_{Max}$  is the amplitude of a selected ultradian CORT oscillation after a perturbation is applied at the maximum of CORT concentration and  $A_{0,ref}$  is the corresponding amplitude of an unperturbed HPA axis when TTS feedback is not considered (i.e. model without relations R30 and R31). **c** Relative change in the ultradian cortisol amplitude  $A_{Max}/A_0$  shows that for all perturbation intensities tested the relative HPA axis response to stress is more intensive when the TTS concentration is high (crosses), than when it is low (triangles/squares). Here  $A_{Max}$  is the amplitude of a selected ultradian CORT oscillation after a perturbation is applied at the maximum of CORT concentration and  $A_0$  is the corresponding amplitude of an unperturbed HPA axis when TTS feedback is considered (i.e. in a model with relations R30 and R31)

ultradian CORT oscillation in an unperturbed HPA axis with TTS feedback (i.e. in a model with relations R30 and R31). Unlike  $A_{0,ref}$ , which is constant,  $A_0$  decreases when the average daily TTS concentration increases, following the same general trend as in Fig. 1c. This analysis revealed that for all intensities of CRH-induced stress tested, the relative HPA axis response is more intensive when the TTS concentration is high (Fig. 4c, crosses vs. triangles/squares). This complex behavior is a direct consequence of the mutual feedback actions between TTS and the HPA axis. It is also in accordance with our previous investigations of the influence of CRH perturbations on HPA axis dynamic states [13, 14, 20], where we have demonstrated that when HPA axis is in a dynamic state with larger amplitudes of

ultradian oscillations it is more resilient to any perturbation. Thus, when the amplitude of ultradian oscillation is larger, the effect of the perturbation is relatively smaller. This is best illustrated by the response of the HPA axis to acute perturbations during the day, when ultradian oscillations are large, and during the night, when they are small [13, 14]. Such behavior of the HPA axis is governed by the dynamic interplay between autocatalytic and autoinhibitory steps that are the underlying core of all our models developed thus far.

In contrast to the observed differences in response to acute stress, kinetic modelling shows that HPA axis response to chronic stress, simulated here as a lasting increase in basal CRH level achieved by increasing the rate constant  $k_2$ , is virtually independent of TTS concentration for physiologically relevant TTS concentrations examined here (Fig. 3k). Thus, reaction kinetic modelling shows that the CRH range in which the HPA axis preserves its dynamic regulation capacity is virtually the same when TTS levels are low (Fig. 3k, circles) and when they are high (Fig. 3k, triangles).

## Discussion and conclusion

TTS is an androgen hormone that is produced in various locations in the human body, most notably in the gonads, but also in the adrenal glands—in females about one quarter of TTS originates from the HPA axis and is produced in the adrenal cortex [27], whereas in males the adrenal cortex contributes to TTS production to a much smaller extent ( $< 5\%$ ). TTS and the HPA axis mutually control one another's activity, wherein TTS suppresses CRH-stimulated HPA axis activity whereas activation of HPA axis has an inhibitory effect on TTS production [28]. While the existence of these bidirectional feedback actions was identified and basic features of their anatomical and biochemical origins were characterized many years ago [29], detailed kinetic mechanisms through which these feedback actions arise and consequences of their action are not yet fully elucidated [30, 31]. Understanding the consequences of these mutually negative interactions is, however, of great importance. HPA axis activity is impaired in many somatic and mental health disorders [32], and gonadal hormones, and TTS in particular, may play an important role in the onset, progression and epidemiology of these diseases as well as in an individual's response to specific pharmacotherapy [33].

Physiologically based reaction kinetic modelling and approaches from dynamical systems theory are useful tools that can help us to better understand the consequences of complex biochemical entanglements. The general aim of kinetic modelling is to systematically reduce the number of dynamical variables to a manageable level and derive a concise representation of the complex system in the form of a low-dimensional stoichiometric network model with good predictive value. Such a model can thereafter help us answer specific questions. In this work, we wanted to understand what the consequences of TTS inhibitory action are on HPA axis dynamics under normal physiology, and how HPA axis response to CRH-induced stress is affected by the feedback action of TTS.

By building on our previous work [11–15, 18], we have developed here a stoichiometric network model that accounts for the inhibitory action of TTS on CRH-induced HPA axis activity and the well-established inhibitory effect of HPA axis activation on secretion of TTS (Table 1). We have demonstrated that this model can replicate experimentally established features of the real HPA axis, such as the physiological levels of all steroid and peptide hormones that constitute the HPA axis (Tables 2 and S3), circadian and ultradian rhythmicity of hormone levels, and the empirically well-established TTS-induced blunting of HPA axis activity (Figs. 1, 2 and 3). These results demonstrate that reaction kinetic modelling can concisely describe the complex and multifaceted effects of TTS on the modulation of HPA axis response to acute CRH-induced stress.

Moreover, kinetic modelling provided important new insights about TTS action on HPA axis activity by showing that TTS increase drives the HPA axis towards a supercritical Hopf bifurcation (Figs. 1 and S2). By showing that a supercritical Hopf bifurcation is being approached for increasing TTS levels, our work offers a better understanding of how TTS level affects HPA axis response to stimuli. When TTS levels are low, the limit cycle around the saddle focus is large, i.e. the amplitude of ultradian oscillations during the active phase is large. Conversely, when TTS levels are high, the limit cycle around the saddle focus is small, i.e. the amplitude of ultradian oscillations during the active phase is small (compare for example time series a with time series e in Fig. 3). As the amplitude of ultradian cortisol oscillations is reduced for increasing TTS levels, perturbations are more likely to be of sufficient strength to produce a disturbance that is larger than the amplitude of the ultradian oscillations under basal (unperturbed) physiological conditions, thereby eliciting a suprathreshold effect (Fig. 4c). Thus, when TTS levels are high, an acute challenge is likely to be of sufficient strength to arouse the HPA axis/neuroendocrine system and may produce a perceptible physiological/behavioral effect, thus offering a possible explanation as to why increased TTS levels are associated with more pronounced behavioral output effects.

Reaction kinetic modelling also showed that while TTS levels affect HPA axis response to acute CRH-induced stress, they did not significantly alter the HPA axis response to chronic stress, as evident from the marginal effect of TTS on the bifurcation diagrams shown in Fig. 3k. In summary, our work shows that stoichiometric network reaction models that describe the kinetics of complex neurochemical transformations are useful tools that can help us to better understand how complex dynamical regulatory networks, such as the nonlinear HPA axis, arise and function under normal physiology and under the effect of internal/external challenges.

**Acknowledgements** Support from the Swedish Research Council, the Knut and Alice Wallenberg Foundation, the Rajko and Maj Đermanović Fund, CMST COST Action CM 1304 “Emergence and Evolution of Complex Chemical Systems”, and the Ministry of Education, Science and Technological Development of the Republic of Serbia, grants 172015 and 45001, is gratefully acknowledged.

**Open Access** This article is distributed under the terms of the Creative Commons Attribution 4.0 International License (<http://creativecommons.org/licenses/by/4.0/>), which permits unrestricted use, distribution, and reproduction in any medium, provided you give appropriate credit to the original author(s) and the source, provide a link to the Creative Commons license, and indicate if changes were made.

## References

1. Stratakis CA, Gold PW, Chrousos GP (1995) Neuroendocrinology of stress: implications for growth and development. *Horm Res* 43(4):162–167
2. Gunnar M, Quevedo K (2007) The neurobiology of stress and development. *Annu Rev Psychol* 58:145–173
3. Herman JP, McKlveen JM, Ghosal S, Kopp B, Wulsin A, Makinson R et al (2016) Regulation of the hypothalamic–pituitary–adrenocortical stress response. *Compr Physiol* 6(2):603–621
4. Hartmann A, Veldhuis JD, Deuschle M, Standhardt H, Heuser I (1997) Twenty-four hour cortisol release profiles in patients with Alzheimer’s and Parkinson’s disease compared to normal controls: ultradian secretory pulsatility and diurnal variation. *Neurobiol Aging* 18(3):285–289
5. Tsigos C, Chrousos GP (2002) Hypothalamic–pituitary–adrenal axis, neuroendocrine factors and stress. *J Psychosom Res* 53(4):865–871
6. Gavrilu A, Peng CK, Chan JL, Mietus JE, Goldberger AL, Mantzoros CS (2003) Diurnal and ultradian dynamics of serum adiponectin in healthy men: comparison with leptin, circulating soluble leptin receptor, and cortisol patterns. *J Clin Endocrinol Metab* 88(6):2838–2843
7. Lightman SL, Conway-Campbell BL (2010) The crucial role of pulsatile activity of the HPA axis for continuous dynamic equilibration. *Nat Rev Neurosci* 11(10):710–718
8. Spiga F, Walker JJ, Terry JR, Lightman SL (2014) HPA axis-rhythms. *Compr Physiol* 4(3):1273–1298
9. Ulrich-Lai YM, Herman JP (2009) Neural regulation of endocrine and autonomic stress responses. *Nat Rev Neurosci* 10(6):397–409
10. Rivier C, Vale W (1983) Interaction of corticotropin-releasing factor and arginine vasopressin on adrenocorticotropin secretion in vivo. *Endocrinology* 113(3):939–942
11. Antoni FA (1986) Hypothalamic control of adrenocorticotropin secretion: advances since the discovery of 41-residue corticotropin-releasing factor. *Endocr Rev* 7(4):351–378
12. Hanukoglu I, Feuchtwanger R, Hanukoglu A (1990) Mechanism of corticotropin and cAMP induction of mitochondrial cytochrome P450 system enzymes in adrenal cortex cells. *J Biol Chem* 265(33):20602–20608
13. Jelić S, Čupić Ž, Kolar-Anić L, Vukojević V (2009) Predictive modeling of the hypothalamic–pituitary–adrenal (HPA) function. Dynamic systems theory approach by stoichiometric network analysis and quenching small amplitude oscillations. *Int J Nonlinear Sci Num* 10(11–12):1451–1472
14. Marković VM, Čupić Ž, Vukojević V, Kolar-Anić L (2011) Predictive modeling of the hypothalamic–pituitary–adrenal (HPA) axis response to acute and chronic stress. *Endocr J* 58(10):889–904
15. Marković VM, Čupić Ž, Maćešić S, Stanojević A, Vukojević V, Kolar-Anić L (2016) Modelling cholesterol effects on the dynamics of the hypothalamic–pituitary–adrenal (HPA) axis. *Math Med Biol* 33(1):1–28
16. Čupić Ž, Marković VM, Maćešić S, Stanojević A, Damjanović S, Vukojević V et al (2016) Dynamic transitions in a model of the hypothalamic–pituitary–adrenal axis. *Chaos* 26(3):033111
17. Čupić Ž, Stanojević A, Marković VM, Kolar-Anić L, Terenius L, Vukojević V (2016) The HPA axis and ethanol: a synthesis of mathematical modelling and experimental observations. *Addict Biol* 22(6):1486–1500
18. Abulseoud OA, Ho MC, Choi DS, Stanojević A, Čupić Ž, Kolar-Anić L et al (2017) Corticosterone oscillations during mania induction in the lateral hypothalamic kindled rat-Experimental observations and mathematical modeling. *PLoS ONE* 12(5):e0177551
19. Stanojević A, Marković VM, Čupić Ž, Vukojević V, Kolar-Anić L (2017) Modelling of the hypothalamic–pituitary–adrenal axis perturbations by externally induced cholesterol pulses of finite duration and with asymmetrically distributed concentration profile. *Russ J Phys Chem A* 91(13):112–119
20. Jelić S, Čupić Ž, Kolar-Anić L (2005) Mathematical modeling of the hypothalamic–pituitary–adrenal system activity. *Math Biosci* 197(2):173–187
21. Rubinow DR, Roca CA, Schmidt PJ, Danaceau MA, Putnam K, Cizza G et al (2005) Testosterone suppression of CRH-stimulated cortisol in men. *Neuropsychopharmacology* 30(10):1906–1912
22. Gear CW (1971) Numerical initial value problems in ordinary differential equations. Prentice-Hall, Inc., Englewood Cliffs, p 253
23. Whirledge S, Cidlowski JA (2010) Glucocorticoids, stress, and fertility. *Minerva Endocrinol* 35(2):109–125

24. Viau V (2002) Functional cross-talk between the hypothalamic–pituitary–gonadal and -adrenal axes. *J Neuroendocrinol* 14(6):506–513
25. Hayes LD, Bickerstaff GF, Baker JS (2010) Interactions of cortisol, testosterone, and resistance training: influence of circadian rhythms. *Chronobiol Int* 27(4):675–705
26. Duke JW, Rubin DA, Daly W, Hackney AC (2007) Influence of prolonged exercise on the 24-hour free testosterone—cortisol ratio hormonal profile. *Medicina Sportiva* 11(2):48–50
27. Guay A, Davis SR (2002) Testosterone insufficiency in women: fact or fiction? *World J Urol* 20(2):106–110
28. Geraghty AC, Kaufer D (2015) Glucocorticoid regulation of reproduction. *Adv Exp Med Biol* 872:253–278
29. Handa RJ, Burgess LH, Kerr JE, O’Keefe JA (1994) Gonadal steroid hormone receptors and sex differences in the hypothalamo-pituitary-adrenal axis. *Horm Behav* 28(4):464–476
30. Kudielka BM, Kirschbaum C (2005) Sex differences in HPA axis responses to stress: a review. *Biol Psychol* 69(1):113–132
31. Goel N, Workman JL, Lee TT, Innala L, Viau V (2014) Sex differences in the HPA axis. *Compr Physiol* 4(3):1121–1155
32. Kt JY, Babic N, Hannoush Z, Weiss RE (2000) Endocrine testing protocols: hypothalamic pituitary adrenal axis. In: De Groot LJ, Chrousos G, Dungan K, Feingold KR, Grossman A, Hershman JM et al (eds) *Endotext*. MDText.com, Inc, South Dartmouth
33. Regitz-Zagrosek V (2012) Sex and gender differences in health. *Science & society series on sex and science*. *EMBO Rep* 13(7):596–603